A comprehensive framework for seismic risk assessment of urban water transmission networks

Sungsik Yoon[a], Young-Joo Lee[b], Hyung-Jo Jung[a],*

[a] Department of Civil and Environmental Engineering, Korea Advanced Institute of Science and Technology, 291 Daehak-ro, Yuseong-gu, Daejeon 34141, Republic of Korea
[b] School of Urban and Environmental Engineering, Ulsan National Institute of Science and Technology, 50 UNIST-gil, Eonyang-eup, Ulju-gun, Ulsan 44919, Republic of Korea

ARTICLE INFO

ABSTRACT

Earthquakes are natural disasters which human beings cannot control, causing significant damage to the economy and society as a whole. In particular, earthquakes affect not only buildings but also lifeline structures such as water distribution, electric power, transportation, and telecommunication networks. The interruption of these networks is critical because it can directly damage the facilities and, at the same time, cause long-term loss of the overall system for society. In recent years, there has been increasing interest in the uncertainties of ground motion, deterioration of pipelines, and interdependency of lifelines. Therefore, it is essential to predict the damage through possible earthquake scenarios and accounting for factors affecting lifeline structures. This study proposes a comprehensive framework to quantify the impact of earthquakes on the connectivity of urban water transmissions. The framework proposes the following steps to predict damage from earthquakes: (1) estimate the ground motion considering the spatial correlation, (2) propose a modified failure probability of buried pipelines considering deterioration, and (3) evaluate the seismic fragility curves of network components and the interdependency among water treatment plants, pumping plants, and substations. For numerical simulations, an actual water network system in South Korea was constructed using graph theory, and the magnitudes and locations of the epicenters were determined based on historical earthquake data. Finally, the reliability performance indicators (e.g., connectivity loss and serviceability ratio) were measured when earthquakes of various magnitudes occurred in the urban area. This framework will enable the prediction of damage from earthquakes and enhance decision making to minimize the extent of damage.

1. Introduction

Significant natural disasters such as earthquakes, landslides, droughts, floods, and hurricanes have occurred in recent times, causing social disruption and economic losses [1,2]. In particular, natural disasters may have a significant influence on complex lifeline systems because social infrastructures in urban areas are highly concentrated. In addition, as the bulk of lifeline facilities are installed underground, it is difficult to recognize and repair the damage, which can lead to a long-term supply stagnation. Recent disasters have highlighted the need to predict damage to lifeline facilities and establish disaster recovery strategies for repairs.

The Pan-American Health Organization (PAHO) [3] analyzed the extent of damage to water distribution networks from natural disasters. Although the damage to the water facilities varied depending on the frequency and intensity of the occurrences, it was reported that

earthquakes have significant influence on water network systems. Earthquakes cause the overall destruction of significant areas of system which results in loss of both life and property, and even more serious secondary damage, including fires following the earthquake, and gas leakages [4]. The probability of a strong earthquake is remote, but once it occurs, the functionality of water network systems could deteriorate. Therefore, it is essential for the earthquake engineering community to conduct a risk assessment of water transmission networks.

The Northridge earthquake in California (1994) and the Kobe earthquake in Japan (1995) caused significant damage to water distribution networks [5]. The Northridge earthquake resulted in 74 instances of damage to main water pipes with diameters greater 600 mm, and 1013 to main water pipes with diameters smaller than 600 mm [6]. In the case of the Kobe earthquake, 23 instances of damage occurred in main water pipes, resulting in disruption of drinking water supplies to approximately 15 million people. In 2016 earthquakes in New Zealand

resulted in a number of problems in critical lifeline structures, that led to both direct and indirect economic losses as residential, commercial, and industrial activities were interrupted. This was a result of the interdependency of lifeline facilities (e.g., water distribution, electric power, transportation, and telecommunication) having an indirect effect on other lifelines (indirect loss) as well as damage to the lifeline itself (direct loss). Therefore, if earthquake damage is not repaired timeously, it could cause not only great discomfort in the lives of local residents, but also significant economic losses.

Various studies have been conducted to predict seismic hazard assessment of infrastructure based on topology-based connectivity. For example, Nuti et al. [7,8] proposed a methodology for seismic safety analysis of electric power, water distribution, and road networks, and they also conducted a seismic evaluation of electric power network at urban level [9]. Esposito et al. [10] worked on the seismic risk assessment of gas distribution networks including the fragility curves of system components, such as metering/pressure reduction stations. Rokneddin et al. [11] presented a finite-state Markov Chain Monte Carlo (MCMC) simulation to evaluate the reliability of ageing highway bridge networks, and proposed a bridge retrofit priority and ranking strategy based on transportation network topology. Ching and Hsu [12] analyzed seismic reliability of actual lifeline networks using Origin-Destination connectivity (O-D connectivity) reliability. With regard to water distribution networks, Yoo et al. [5] proposed a model to conduct the seismic hazard assessment of J-city and I-city in South Korea considering water network facilities such as water storage tanks and water pumping plants. Fragiadakis and Christodoulou [13], and Fragiadakis et al. [14] conducted a seismic reliability assessment of the Limassol water supply network in Cyprus by introducing the modified repair rates equation to account for the degradation of distribution pipelines. Moreover, Christodoulou et al. [15] proposed a methodology for assessment of Water Distribution Network (WDN) system based on network topology and component analysis. Osorio et al. [16] evaluated the seismic response of critical interdependent networks between water distribution and electric power networks, and proposed a recovery strategy to mitigate damage. In addition, Poljanšek et al. [17] presented a model to consider the interdependence of gas and electric power networks and conducted research on power losses in Europe according to the coupling strength. Regarding the non-simulation-based algorithm, Lee et al. [18] evaluated the post-hazard flow capacity of a road network considering the deterioration of bridges in Sioux Falls, USA, by means of a non-sampling-based matrix-based system reliability (MSR) method [19,20]. Song and Ok [21] proposed a multi-scale system reliability method to evaluate gas distribution networks in Shelby County, Tennessee, USA, using the MSR method as well. In addition, Lim and Song [22] proposed a selective recursive decomposition algorithm to evaluate risk assessment of water networks subjected to spatially correlated ground motions.

Previous studies have suggested an effective way to predict and assess damage from earthquakes. However, even if such analytical methods were developed, only limited studies have combined all the analytical methods. For example, Fragiadakis and Christodoulou [13] studied seismic reliability assessment considering the fragility of water treatment plants, water storage tanks, and pumping plants, but excluded water transmission network systems. Yoo et al. [5] excluded the interdependency of lifeline facilities and the spatially correlated ground motion prediction equation (GMPE) in their study. In other studies numerical simulations considering deterioration of pipelines were not conducted. To overcome the limitations of previous studies, this study proposes a comprehensive framework that incorporates the spatially correlated ground motion, deterioration of pipelines, and interdependency of water and electric power networks, as well as the fragility of water treatment plants, water storage tanks, and pumping plants. An actual water transmission network in A-city, South Korea, was used as the target region for applying the comprehensive framework, as A-city is subjected to frequent earthquakes.

The organization of this paper is as follows. Section 2 introduces the theoretical background of the comprehensive framework including network analysis, prediction of ground motion, damage to deteriorated pipelines, fragility curves of other facilities, and interdependency between water and electric power networks. In Section 3, we propose a comprehensive framework for seismic risk assessment of urban water networks. Section 4 describes an actual water transmission network in A-city in South Korea, and presents the results of the seismic risk analysis in accordance with earthquake magnitude, elapsed time, and interdependency. Finally, Section 5 concludes this study and recommends future study directions to add to and improve on this study.

2. Theoretical background

2.1. Network analysis

2.1.1. Graph theory

Graph theory is a powerful mathematical tool for easy control of complex network data. The graph theory comprises nodes (junctions) and edges (links), denoted by V and E, respectively, and can be expressed as $G = (E, A)$. The graphs are divided into directed and undirected graphs according to whether the direction between the initial node ($v1$) and end node ($v2$) is unidirectional or bidirectional, and a mixed graph exists when two graphs coexist together. The connectivity of the graph represents the topological structure of the network, and the entire network is represented by an $N \times N$ adjacency matrix A, where N is the total number of nodes in the network. The component of the adjacency matrix A is $A_{ij} = 1$ if the connection between nodes i and j is possible, otherwise 0. Using graph theory, it is possible to identify the shortest path and connectivity between sources and the sink node. In addition, it can be effectively used in a large network because it can easily reflect the destruction of links resulting from external disturbances such as earthquakes. Fig. 1 shows an example of a simple network and adjacency matrix.

2.1.2. Performance indicator

Once the failure probabilities of all water network facilities are known, the performance of the entire network can be evaluated. Various approaches for evaluating network performance can be utilized, depending on requirements of the user (i.e., connectivity and flow reliability). A proper indicator must be determined to enable accurate performance measurement, as it depends on network size, type, and topology of the graph. Therefore, it is important to define a failure status of the network by setting parameters that have a significant effect on the network. As a simple example, success and failure can be categorized depending on whether or not the water from the source node can reach the sink node. In addition, it is also possible to evaluate the importance of each storage tank (sink) considering the number of inhabitants supplied from the water treatment plant (source). Once the quantified network assessment methods are determined, the performance indicators can be evaluated accurately.

In this study, two performance indicators, connectivity loss (CL) and serviceability ratio (SR), were used to evaluate the network performance from source to sink. Both indices are vulnerability analysis based on connectivity. Typically, two quantified indicators can be classified into minor, moderate, and major damage states according to
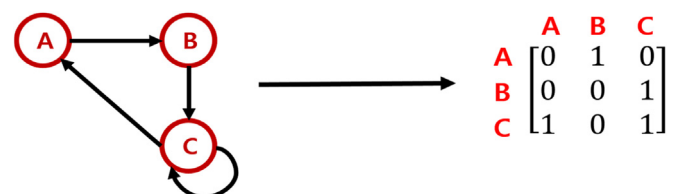

Fig. 1. Example of simple network and adjacency matrix.

performance of 20%, 50%, and 80%, respectively, and it is possible to evaluate the status of systematic network. From quantified indicators, it is possible to evaluate the performance of waterworks and this is easily adapted to other lifeline structures.

The CL is the connectivity index between the source node i and the sink node j which is expressed as the ratio of connectivity before and after earthquake. The definition of CL is shown in the following equation, which is similar to the equation Poljansek et al. presented in 2011 [17].

$$CL = 1 - \left\langle \frac{N_{i,Damaged}}{N_{i,Intact}} \right\rangle_i \tag{1}$$

where $N_{i,Damaged}$ is the number of sink nodes connected to source node i after an earthquake, $N_{i,Intact}$ is the number of sink nodes connected to source node i in the intact network, and the operator $\langle \bullet \rangle_i$ represents the average value of connectivity ratio of all source nodes i.

The SR measures the number of transmission nodes accessible from the source node. The definition of SR can be defined by the following equation, which is similar to the equation Adachi and Ellingwood proposed in 2008 [23]. The proposed SR equation considers all distribution nodes, but, as there is no flow rate in the transmission pipe, the SR is calculated using only the sink node.

$$SR = \frac{\sum w_j X_{i,j}}{\sum w_j} j = 1, ..., N_s \tag{2}$$

where w_j is the total water demand from the source, N_s is the number of storage tanks, and $X_{i,j}$ is the probability of success of the water supply from the source to the sink from the Bernoulli trial. If the source node i and sink node j are connected, $X_{i,j} = 1$ otherwise, $X_{i,j} = 0$.

2.2. Spatially correlated seismic attenuation law

2.2.1. Ground motion prediction equation

The ground motion is the process of energy radiating from the source to the ground surface during the rupture. Various ground motions can be generated according to the seismic propagation and geological characteristics. Traditionally, the ground motion is predicted by a probability distribution of seismic intensity measure (IM) which is conditionally selected considering variables such as seismic source, seismic propagations path, and local site environments [24]. For considering complex physical phenomenon, a GMPE was proposed by simple mathematical expressions [25–27]. The representative parameters for describing a GMPE are magnitude of the earthquake, the distance from the source to the site, fault type, and site class of ground [24]. The typical ground motion is given as [28–30]:

$$LogY_{ij}(T_n) = Log\overline{Y}_{ij}(M_j, \overline{R}_{ij}, \lambda_{ij}, T_n) + \eta_j(T_n) + \varepsilon_{ij}(T_n) \tag{3}$$

where $Y_{ij}(T_n)$ is the ground motion parameter at the i-th site because of the j-th seismic event with vibration period T_n, M_j is the magnitude of the j-th earthquake, R_{ij} is the distance between the source and site, λ_{ij} is other factors that influence the ground motion, and $\overline{Y}_{ij}$ describes the median value of the ground motion. The last two terms of η_j and ε_{ij} indicate the inter- and intra-events, respectively, which represent the uncertainty of the ground motion. These two parameters are independent from each other and follow the normal distribution with a zero mean (μ_η, $\mu_\varepsilon = 0$) and standard deviation (σ_η, σ_ε). The two terms are described in detail in Section 2.2.2.

As GMPE is characterized by propagation paths and local site conditions, therefore, an appropriate GMPE should be adopted for specific studied areas. It has been widely reported in the literature that buried pipelines exhibit vulnerability to the peak ground velocity (PGV), and other facilities such as water treatment plants, and pump stations are vulnerable to the peak ground acceleration (PGA). In this study, the GMPE for PGV proposed by Wang and Takada [31] and the PGA proposed by Kawashima et al. [32] were utilized to consider the seismic

wave propagation in a water distribution network. The two equations are as follows:

$$Log(PGV) = 0.725M + 0.00318H - 0.519 - 1.318log(R + 0.334e^{0.653M}) \tag{4}$$

$$PGA = 403.8 \times 10^{0.265M} x(R + 30)^{-1.218} \tag{5}$$

where M is magnitude of the earthquake, H is the focal depth (km), and R is epicentral distance (km).

2.2.2. Spatial correlation

The GMPE proposed in Section 2.2.1 is able to calculate the median value of the ground motion. However, as the GMPE parameters have an uncertainty, it is essential to accurately predict the ground motion considering the residual terms. The residual terms of the GMPE can be expressed as inter-event (between earthquakes) and intra-event (within the earthquake) residuals [27]. The inter-event indicates that the released energy can be varied during the rupture even if the different seismic waves are propagated in the same path. The intra-event indicates that the propagated energy can be varied because of different seismic wave paths and geotechnical environments [33]. Therefore, inter-event residuals generate constant spatial values (overall increase or decrease), while intra-event residuals have spatially correlated ground motions depending on the propagated paths.

There are numerous spatial correlation models with respect to seismic regions, including for California [30], Europe [34,35], Taiwan [31,36], and Japan [31,37,38]. As the spatial correlation is derived according to the geotechnical characteristics, an appropriate correlation model should be adopted for specific studied areas. In this study, the intra-event correlation equation proposed by Goda and Hong [30] was used for considering the spatially correlated ground motion, as the seismic design code of a buried pipeline in South Korea was released based on the Californian regions. An equation for considering the total correlation can be expressed as [36]:

$$\rho_{Total} = \frac{\sigma_\eta^2}{\sigma_\eta^2 + \sigma_\varepsilon^2} + \frac{\sigma_\varepsilon^2}{\sigma_\eta^2 + \sigma_\varepsilon^2}\rho(\Delta_{ij}) \tag{6}$$

where

$$\rho(\Delta_{ij}) = e^{(-0.509\sqrt{\Delta})} \tag{7}$$

is the intra-event correlation function, Δ_{ij} is distance between the i-th site and the j-th site, and σ_η and σ_ε are the inter- and intra-event residuals, respectively, which are predefined terms.

2.3. Seismic vulnerability analysis of networks

2.3.1. Deterioration of water pipelines

The US Federal Emergency Management Agency (FEMA) and American Lifelines Alliance (ALA) presented the failure probability of buried pipelines [39,40]. According to the report, the bulk of historical earthquake records show the failure probability of buried pipes based on the repair rate (number of breaks per unit length). The repair rate is calculated based on the regression curve, which represents the number of pipe breaks due to ground motion. Typically, PGV and peak ground deformation (PGD) are known as the representative IM that affects pipeline damage. The PGV represents a strong ground motion by seismic wave propagation, whereas the PGD represents the effect on landslides, liquefaction, ground settlement, and fault crossing [13]. In this study, the effect of ground motion was investigated by selecting the PGV as the IM. In the HAZUS-MH manual, the repair rate of the i-th brittle pipeline (cast iron, concrete, and cement pipes) is calculated by the following formula:

$$RR_i(breaks/km) = \kappa(PGV_i)^\tau \tag{8}$$

where PGV_i is ground motion of midpoint of the i-th pipeline, and κ and τ

are the scaling and exponent parameters, respectively. For ductile pipelines (steel and ductile iron), the average repair rate is reduced by 30% compared to brittle pipelines. By substituting the calculated repair rate into the fragility model, the failure probability of the i-th buried pipe can be obtained as follows:

$$P_{f,i} = 1 - e^{-RR_i L_i} \qquad (9)$$

where RR_i and L_i are the repair rate and length of the i-th pipeline, respectively. Depending on the extent of damage, the failure probability of pipelines can be classified as either complete damage or leakage damage that could lead to water supply disruption. According to technical reports, 15–20% of the failures are total break damage, while 80–85% are reported as leakage damage [41]. Some researchers conducted seismic fragility curve analysis of gas and liquid pipeline with respect to different damage states and risk states [42–44]. However, since the seismic hazard assessment is conducted based on connectivity analysis (break or not) in this study, the repair rate proposed by FEMA was utilized.

As the proposed fragility model follows the Poisson process, past events have memoryless properties that do not affect the present. Therefore, the probability of pipeline failure is determined only by IM, and the aging effect from structural deterioration is not taken into account. In this study, the survival function was utilized to consider the deterioration of buried pipelines. Survival analysis is a method of predicting the expected or residual lifetimes of a structure based on past data [45,46]. The shape of the survival function is shown to be dependent on a number of factors, including the number of previous breaks (NOPB), material type, incident type, and diameter range [47,48]. Fragiadakis and Christodoulou [13] conducted seismic reliability assessments using the NOPB-based survival analysis of the Limassol water supply network in Cyprus. They proposed a modified repair rate equation by considering the ratio of intact and damaged survival functions. The modified repair rate and failure probability can be expressed as:

$$\overline{RR}_i = \frac{S(t)_{Intact\ pipe}}{S(t)_{Damaged}} \times RR_i \qquad (10)$$

where $\overline{RR}_i$ is the modified repair rate of the i-th pipeline, $S(t)_{Intact\ pipe}$ and $S(t)_{Damaged}$ are survival functions of intact (NOPB = 0) and damaged pipelines (NOPB ≠ 0), respectively, and t is the elapsed time since being buried. By substituting the calculated modified repair rate into Eq. (9), the modified failure fragility model is defined as follows:

$$\overline{P}_{f,i} = 1 - e^{-\overline{RR}_i L_i} \qquad (11)$$

where $\overline{P}_{f,i}$ is the modified failure probability and repair rate of the i-th pipeline.

However, the survival function proposed by Fragiadakis and Christodoulou [13] is not appropriate for water transmission network due to different characteristics of pipelines (different diameters and materials). Therefore, this study utilized the survival function of the water transmission network which was proposed by Park et al. [49]. In their study, NOPB is not considered as a parameter of the survival function, and they assumed that all pipes deteriorate equally over time (NOPB ≠ 0), which means that $S(t)_{Intact\ pipe}$ is always defined as 1, while $S(t)_{Damaged}$ decreases over time depending on the pipeline properties. The parameters of the survival function, comprising pipe diameter, length, age, and material (steel or cast iron) of the South Korea transmission pipes, are suitable for this case study. Fig. 2 shows the survival function of 600 mm diameter and 500 m long cast iron and steel pipes. The survival probability of the cast iron pipeline decreased rapidly after 25–30 years of use, and the steel pipes did not significantly deteriorate even after 30 years of use. The results indicate that steel pipes have a greater survival probability than cast iron pipes that is in agreement with statistics from waterworks (see Fig. 2).

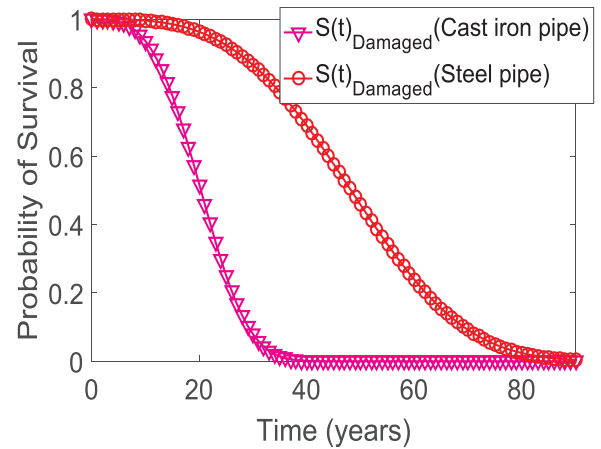The survival function proposed by Park et al. [49] was used to

Fig. 2. Survival function of water transmission pipe with 600 mm diameter and 500 m length.

estimate the modified repair rate $\overline{RR}_i$ and the modified failure probability $\overline{P}_f$. As $S(t)_{Intact\ pipe}$ is assumed to be 1, the modified repair rate is expressed only as a function of the existing repair rate and $S(t)_{Damaged}$. From the modified repair rate, the modified failure probability is calculated by using Eq. (11). Fig. 3 compares existing failure probabilities proposed by FEMA with modified failure probabilities. The modified failure probability is significantly greater than the existing failure probability when the buried time increases from 20 to 30 years. As the survival probability of steel pipes is more reliable than that of cast iron pipes, the failure probability of cast iron pipes increased significantly with increasing time, however, the failure probability of steel pipes did not vary substantially (see Fig. 3). Note that life expectancy of steel and cast iron pipes utilized in the South Korea waterworks association is approximately 30 years.

2.3.2. Other facilities

A water transmission network comprises water treatment plants, water storage tanks, and water pumping plants. For water network facilities, the PGA is taken as the IM parameter that affects structural damage. The failure probability of facilities is modeled as a log normally distributed function, which is determined by the median and standard deviation of the ground motion. Damage states are classified into five states depending on performance of the structures: 1) no damage state; 2) slight/minor damage state: localized damage and minor cracks; 3) moderate damage state: malfunction of system with minor loss; 4) extensive damage state: malfunction of system with severely damaged; 5) complete damage state: collapsed. In this study, the damage state is assumed to be an extensive damage state which implies that the damage state is more severe than a short-term malfunction but less than a complete collapse.

The water treatment plant purifies the intake water and supplies it to the storage tank. HAZUS-MH classified water treatment plants into three types according to their purification capacity: small water treatment plant: 10 *mgd* < capacity ranging < 50 *mgd*, medium water treatment plant: 50 mgd < capacity ranging < 200 *mgd*, and large water treatment plant: capacity ranging > 200 mgd, where *mgd* is the millions of gallons per day. The pumping plant increases the flow pressure to supply water from low to high areas. The pumping plant facility comprises a small pumping plant (capacity less than 10 *mgd*) and a medium/large pumping plant (capacity greater than 10 mgd). Finally, the storage tank stores the purified water supplied from the water treatment plant and delivers the water to each household through distribution pipelines. The storage tanks are of steel, concrete, or wood materials, and the storage capacity is typically 0.5–2 mgd. The fragility curves of each structure can be classified as either anchored or

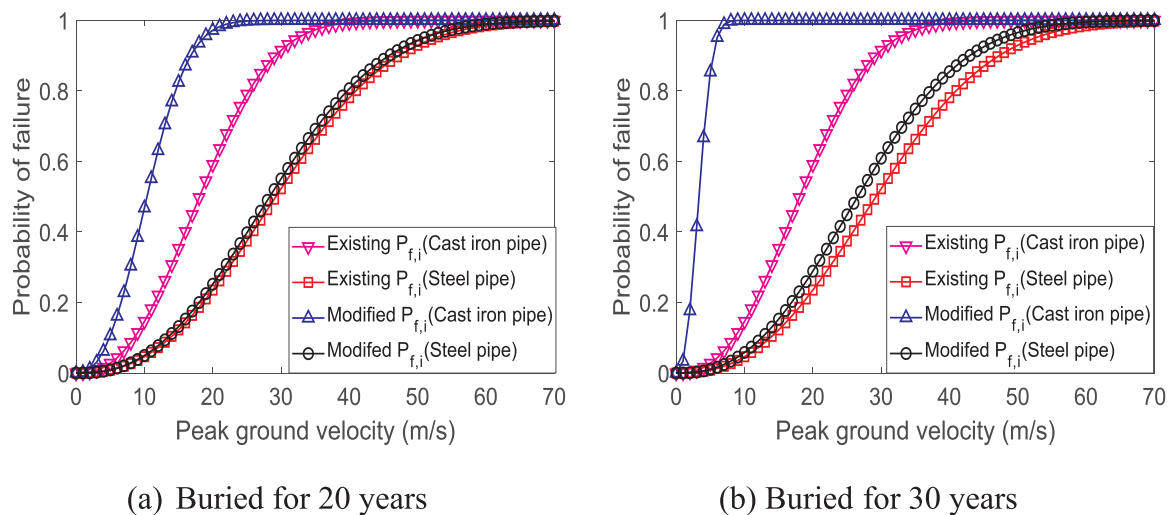(a) Buried for 20 years   (b) Buried for 30 years

Fig. 3. Comparison of failure probability between existing repair rate and modified repair rate for pipelines buried for (a) 20 years, and (b) 30 years (600 mm diameter and 500 m length).

unanchored, depending on whether it is seismically designed or a standard design. Fig. 4 shows the failure probability of water treatment plants, pumping plants, and storage tanks as functions of various treatment capacities and material types.

2.3.3. Interdependent facilities

In an actual network, lifeline facilities are closely related to other lifeline components. For example, the electric power network is supplied with fuel from the gas network to operate the generator, and the water network supplies water to the power generator facility to reduce
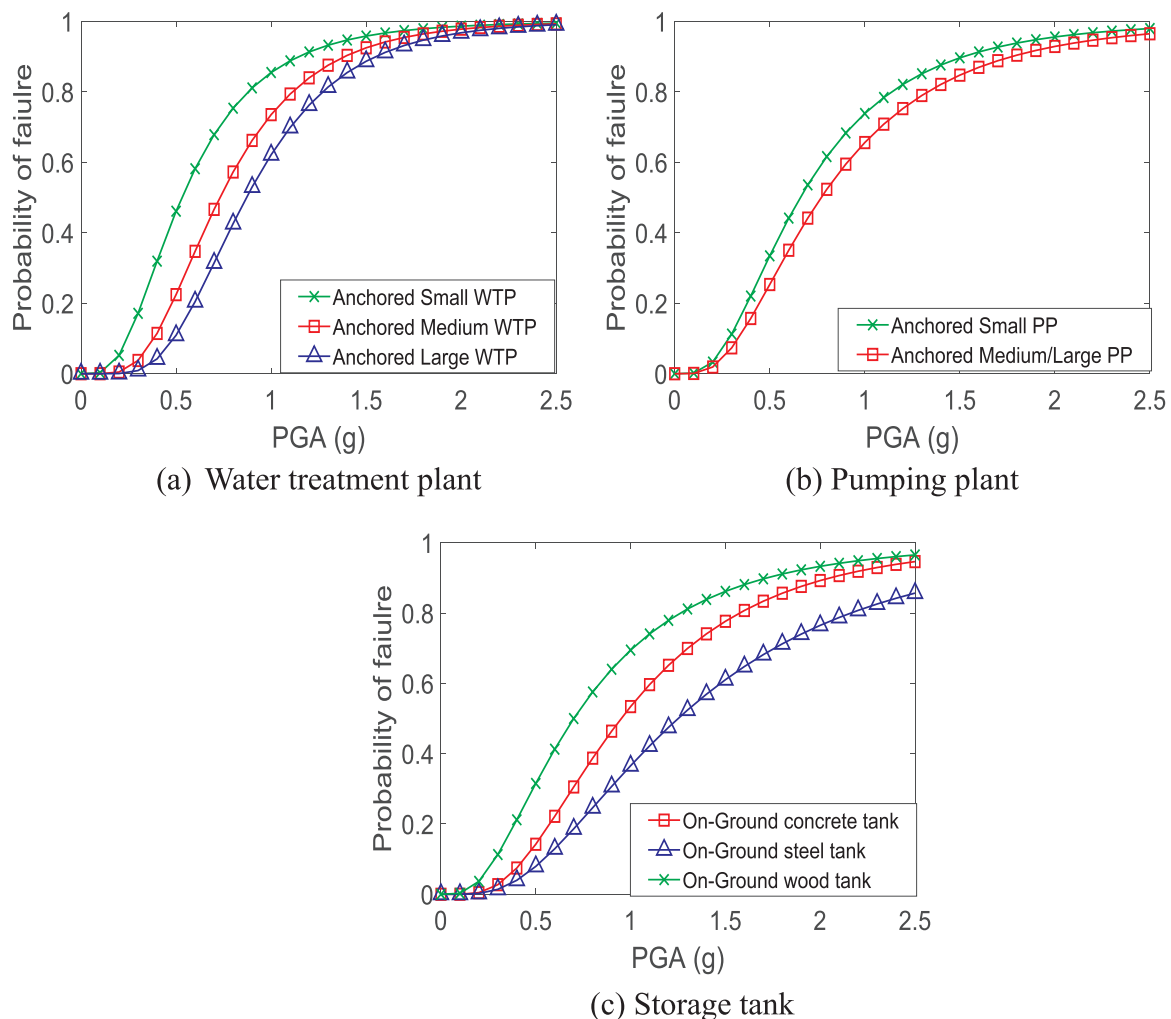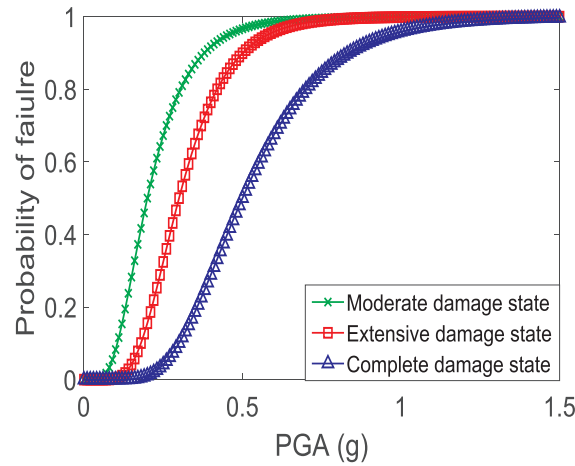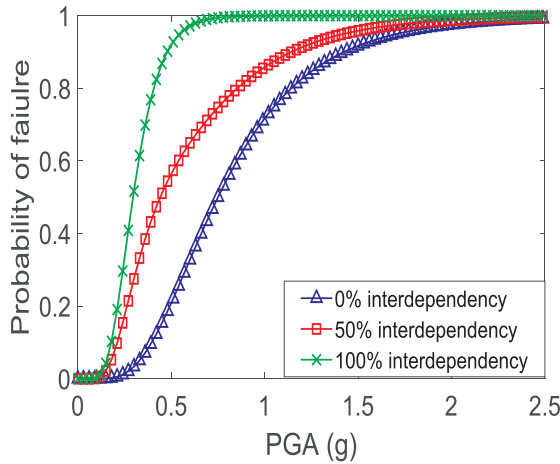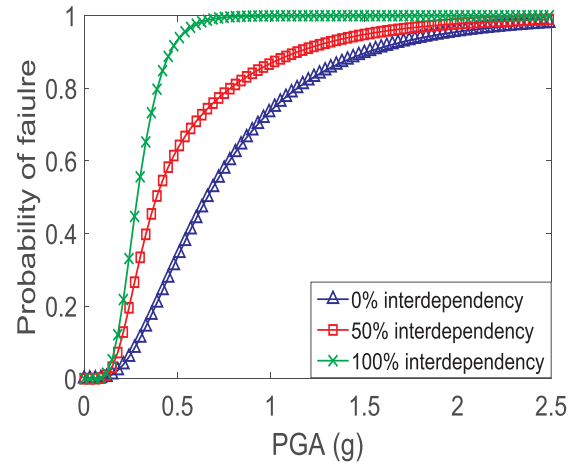

(a) Water treatment plant   (b) Pumping plant

(c) Storage tank

Fig. 4. Failure probability of (a) water treatment plant, (b) pumping plant, and (c) storage tank.

(a) Electric power substation

(b) Medium water treatment plant

(c) Small pumping plant

Fig. 5. Failure probability of (a) electric power substation, (b) medium water treatment plant, and (c) small pumping plant, considering effect of interdependency.

the gas emissions. In addition, electric power is used to operate the pumping and water treatment plants. As all lifeline facilities have an effect on each other, the interdependency-based approach provides more reliable results.

In this study, we consider two interdependent facilities where the water treatment and pumping plants are supplied with electric power from a power network. The water distribution network could suffer direct destruction from ground motions, but indirect disruptions could occur because of power supply interruptions. The failure probability of substations is defined as the extensive damage state in Fig. 5(a), and the strength of the coupling of the two facilities can be expressed using conditional probability. When the j-th substation is destroyed, the failure probability of the i-th water facility can be expressed as follows:

$$P(T_i^{interdep}|S_j^{seismic}) = p_{T_i|S_j} \text{ for all node adjacent to jnode} \quad (12)$$

where $S_j^{seismic}$ is the failure probability of the j-th substation, and $T_i^{interdep}$ is the failure probability of the i-th water facilities because of interdependency. The coupling strength of the two facilities are between 0 and 1, with 0 for independent coupling strength and 1 for complete coupling strength. Fig. 5(b) and (c) show the failure probabilities of the water treatment and pumping plants as coupling strength increases from 0 to 1. Interdependency does not have a significant effect at low

PGA, however, interdependency has a significant influence on the failure probability with increasing PGA.

3. Comprehensive framework: probabilistic reliability model

In this section, we propose a comprehensive framework (probabilistic reliability model) that combines the methods discussed in Section 2. A comprehensive framework is critical for decision making and management planning to design and evaluate a water transmission network. The proposed framework will enable the prediction of system performance against earthquakes as well as help in preparing a management plan for a stable water supply.

The probabilistic reliability model presents the performance of network topology through a Monte Carlo simulation (MCS). An example of evaluating a network assessment using MCS can be found in references [23,50–53]. Fig. 6 presents a flowchart of a probabilistic reliability model implemented in this study, and the basic process of the model is as follows:

(1) Construct the network topology based on the Graph theory to simplify the complex water networks with junctions (node) and links (edge). Network data include an $N \times N$ adjacency matrix, the position of junctions, and nodes that make up the edge.
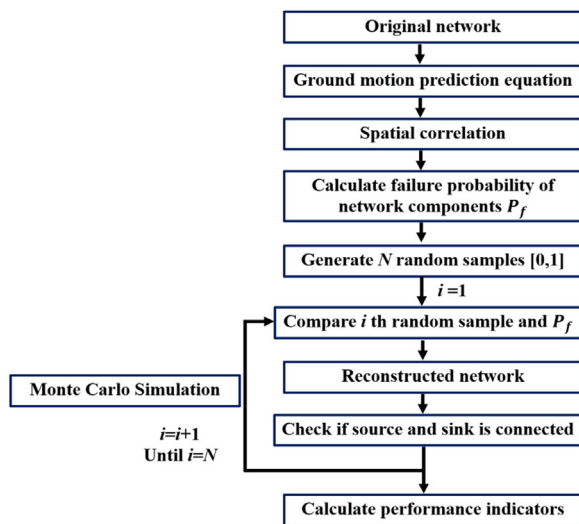
Fig. 6. Flowchart of comprehensive framework utilized in study.

Fig. 7. Number of path between source and sink nodes.

(2) Determine the location of the epicenters, focal depth, and earthquake magnitudes from historical data or potentially earthquake-prone regions.
(3) Estimate the spatially correlated GMPE considering uncertainty of the ground motion model. The GMPE should be determined as a model that represents the characteristics of the geotechnical environment.
(4) Calculate the failure probability of deteriorated pipelines considering diameter, length, age, and materials.
(5) Calculate the failure probability of network components (water treatment plants, pumping plants, water storage tanks, and electric power substations) considering interdependencies between water and electric power networks.
(6) Generate N random correlated samples between 0 and 1 using the inverse transform sampling method [54,55], and determine the state of the structure by comparing the i-th random number with the structure failure probability. The component is damaged if the random number is smaller than the failure probability calculated in steps (4) and (5), otherwise the pipeline maintains an intact state.
(7) Depending on the state of the structure, it is stored as binary state vectors of 0 (intact state) or 1 (damage state). From the stored binary state vector, the modified network is reconstructed by removing the link on the existing network.
(8) From the reconstructed network, check if the source node and sink node are connected using the deep first search algorithm [56–58]. This is also stored as binary state vectors of 0 (failure) or 1 (connected). Return to step (6) and repeat steps (6)–(8) until the $(i + 1)$-th random generator equals the defined MCS number N.
(9) Calculate the performance indicators (CL and SR) by using the binary state vectors calculated in step (8).

Steps (6)–(8) are performed in each MCS run, and this provides a set of performance indicators with certain hazard levels through repeated executions. Each set of performance indicators are calculated depending on earthquake magnitude, buried time, and extent of interdependency.

4. Seismic risk analysis of water transmission network

4.1. Description of water transmission network of A-city

The primary aim of this study is to obtain A-city water transmission network data, location information of the 154 kV substations, and a system diagram of substations supplying to water network facilities.
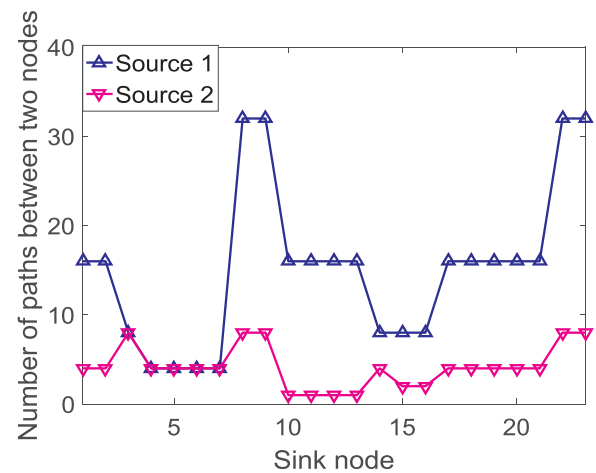
The source data was provided from A-city waterworks business headquarters, and the network data presented here shows the post processing results of the source data.

The waterworks of A-City supplies water to 1,150,215 people in an area of 1057 km² through 285 nodes (258 transmission nodes) and 291 edges (276 transmission edges). The total length of the edges (water pipelines) is 151.7 km, and the pipelines diameter is greater than 600 mm. Two types of material were used: steel pipes (10%), and cast iron pipes (90%). The steel pipes were typically used for the aqueduct pipelines, and the cast iron pipes for the transmission pipelines. The network system comprises two water treatment plants (source), 23 storage tanks (sink), 15 pumping plants, and 10 substations that supply electric power to the pumping and water treatment plants. The electric power is supplied through 154 kV substations with a reduced voltage of 22.9 kV. Fig. 7 represents a number of path between sources and sinks in water transmission network of A city. In addition, there are 7 loops in the transmission pipeline network and 6 loops in the aqueduct pipeline network. For more detailed information, the network map of A city is represented in Fig. 9.

The scope of this study is to evaluate whether water supply is possible from the source to the sink. The procedure of supplying water from the source to the sink in A-city is shown in Fig. 8. Raw water is first supplied to the water treatment plant through aqueduct pipelines. Once it is purified, the water can be distributed to the storage tanks through transmission pipelines and pumping plants. Therefore, in order to supply water to the water storage tank, not only the pipeline but also the water transmission network component should be operating normally. In addition, the 154 kV substations are considered to represent the interdependency effects between the water network and the electric power network.

In this study, we evaluate the seismic reliability of the water transmission network of A-city using the probabilistic reliability model. The water network map of A-city is shown in Fig. 9. The epicenter was chosen as the location of an historical earthquake of 5.8 magnitude that was both the closest and largest earthquake occurred in A-city. Because of security concerns, this study does not disclose specific information about A-city. The purpose of this study is limited to identifying the possibility of seismic risk assessment using the proposed comprehensive framework, so the probabilistic seismic hazard analysis such as line or area source was not considered. For the numerical example, earthquakes with magnitudes in the range of 5.0–7.0 were considered, and the focal depth was assumed to be 10 km. From the results of the numerical simulation, we measured the seismic risk in terms of CL and SR with respect to various earthquake magnitudes, elapsed time, and interdependency. The comprehensive framework presented in Section 3 was used for the numerical simulations.
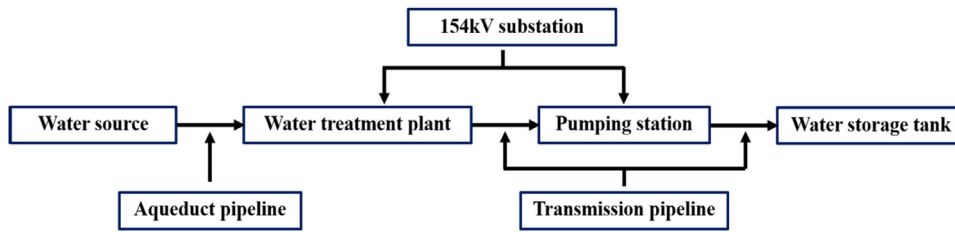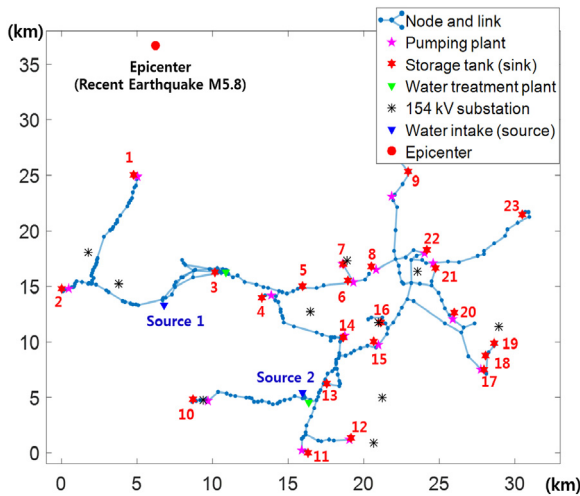
Fig. 9. Representation of water transmission network of A-city using graph theory.

4.2. Results of network response

The first case study evaluated the seismic risk assessment of the water transmission network without considering the electric power network. We first considered the connectivity between the source and sink from the earthquake, taking into consideration the effects of aqueduct and transmission pipeline degradation. To perform the numerical analysis, a magnitude 5.0–7.0 earthquake was generated and the spatially correlated PGA and PGV were calculated using the GMPE presented in Eqs. (3)–(7). In the case of deterioration of the pipeline, we considered the aging of water pipes to be 0–30 years using Eqs. (10) and (11). Note that the seismic design criteria for water network systems in South Korea is a magnitude 5.7–6.4 earthquake with a service life of the transmission pipe of approximately 30 years.

In order to represent the vulnerability of the water system, the fragility surfaces were plotted with respect to earthquake magnitude and elapsed time. A total of 10,000 MCS runs were performed for each case, and the results are presented in Figs. 10–12. In the water network of A-city there are two source nodes and one sink node, therefore, the fragility surfaces were classified into three scenarios: source 1-sink, source 2-sink, and two sources-sink. Figs. 10–12 show the CL and SR surfaces of the water transmission network with the earthquake magnitude and the elapsed time after being buried. When supplying water from source 1, most of the purified water was delivered to sinks of magnitude 5.0 (CL $\cong$ 0, SR $\cong$ 1: no damage). Even with the magnitude 6.0 earthquake, CL and SR were measured as 0.25 and 0.75 (minor state), respectively, however, as the magnitude of the earthquake increased from 6.0 to 7.0, CL increased significantly to 0.52 and SR decreased significantly to 0.47 (moderate state). In the case of a magnitude 7.0 earthquake, the degradation of the pipe because of the elapsed time had a significant influence on the network system. After 20–30 years after being buried, the CL performance of the network increased significantly from 0.6 to 0.82, whereas the SR performance decreased rapidly from 0.39 to 0.17 (major state).

The second scenario is the case where water is supplied from source 2. In this scenario, it is evident that the network becomes more reliable as the water treatment plant is located farther from epicenter than in the first scenario. When comparing Fig. 10 with Fig. 11, it can be seen that CL tends to decrease and SR tends to increase overall. Specifically, when the earthquake magnitude and the time were 7.0 and 30 years, respectively, the CL and the SR varied by 0.12 and 0.08, respectively, which renders the state of the system more stable (major → moderate). The final scenario is an evaluation of the system considering two sources. For this scenario, the network becomes more reliable than for the previous two cases, as two sources are considered. Fig. 12 shows a relatively more reliable fragility surface when compared to Figs. 10 and 11. Even in cases where the earthquake magnitude was 7.0 and the time was 30 years, the CL was smaller than 0.4 and the SR was greater than 0.6, that indicates that the system was in a minor-moderate damage state.

4.3. Results of network response considering power network

The second case study assessed the stability of the water transmission network considering interdependency between two networks. Based on the scenario introduced in Section 4.2, the effect of the electrical power supply was further considered. As discussed in Section 2.3.3, substations transmit electric power to water treatment and pumping plants. Therefore, if the substation is damaged, it becomes difficult to supply the purified water to the network system. As shown in Fig. 8, electric power is supplied from substations which are adjacent to the water treatment and pumping plants.

Figs. 13–15 show the CL and SR surface of the water transmission network depending on the extent of interdependence when the system is subjected to an earthquake of magnitude 5.0–7.0. The dependency among the components is based on the conditional probability given in Eq. (12), that is considered to increase the strength of the coupling of 0, 0.5, and 1. The conditional probability $p_{T_i|S_j} = 0$ represents the independent environment among the network components, whereas $p_{T_i|S_j} = 1$ represents the complete interdependence relationship among the network systems. It can be seen in Figs. 13–15 that the system fragility increases as the coupling strength increases from 0 to 1. The performance of the water network system became less reliable with increasing earthquake magnitude and elapsed time (discussed in Section 4.2). In addition, as the interdependency of the network components increased, it had a significant influence on the fragility surface of the system. Compared to the case without interdependency, the SR decreased by approximately 0.06–0.11 (interdependency = 0.5) and 0.09–0.15 (interdependency = 1), whereas the CL increased by approximately 0.05–0.1 (interdependency = 0.5), and 0.08–0.14 (interdependency = 1) when the earthquake magnitude was 7.0 (see Fig. 13). In the case of the storage tank supplied from source 2 and two sources connectivity, the fragility surface of CL decreased and SR increased compared to the fragility surface of Fig. 13, as the water treatment plant was located farther from the epicenter.

5. Discussion

In the first case study, the network response of independent systems was considered. When the earthquake magnitude was smaller than 6.0,
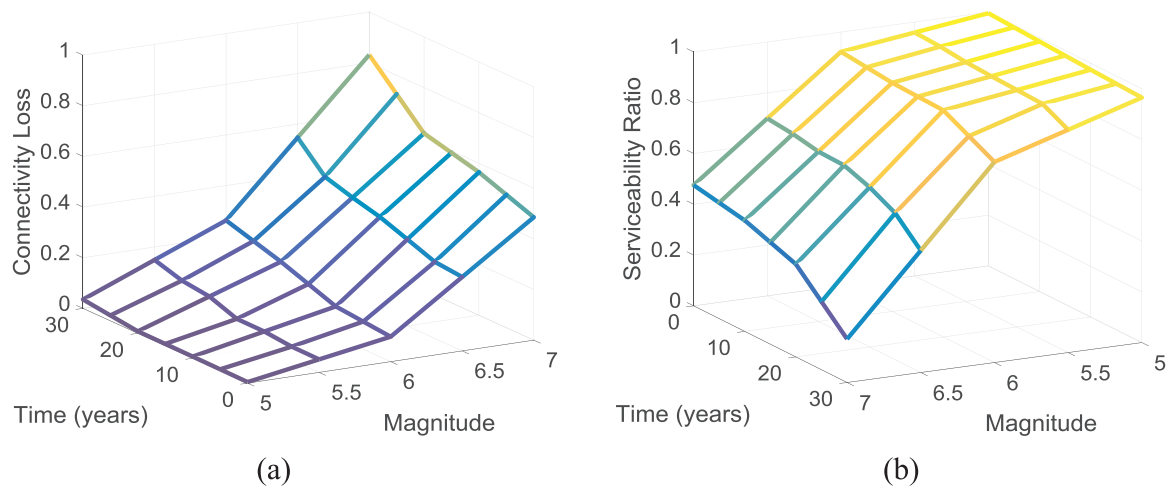
Fig. 10. Fragility surface of independent water transmission network (source 1–sink connectivity): (a) CL, and (b) SR.
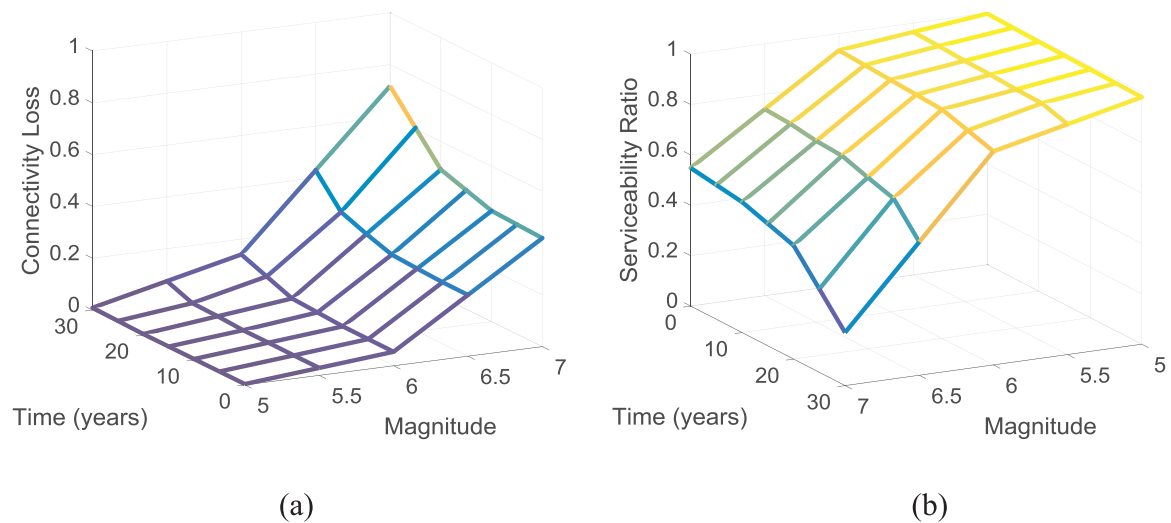

Fig. 11. Fragility surface of independent water transmission network (source 2-sink connectivity) (a) CL (b) SR.
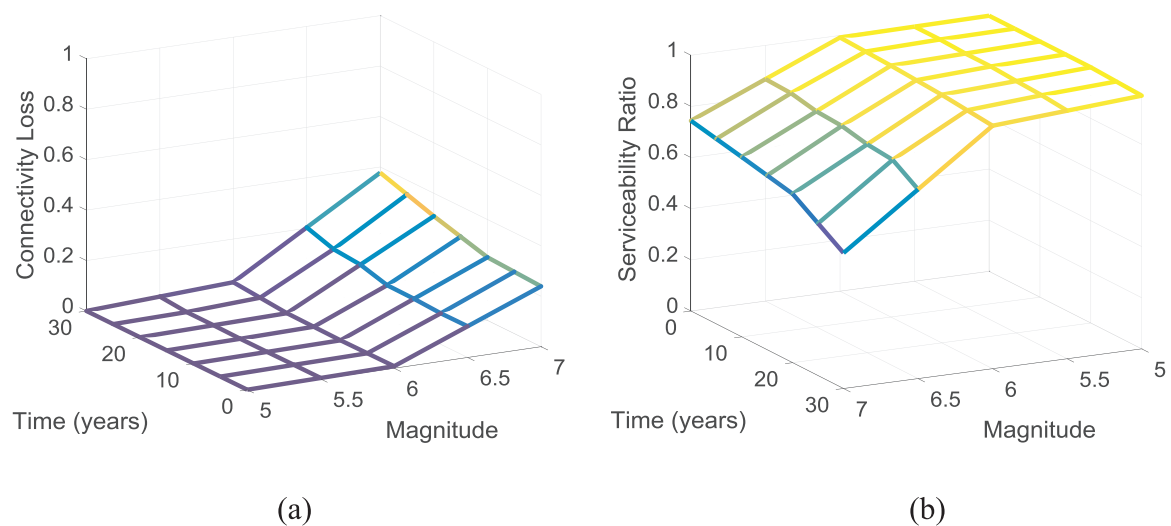

Fig. 12. Fragility surface of independent water transmission network (two sources-sink connectivity) (a) CL (b) SR.

the network system exhibited a minor damage state, and the degradation of the buried pipe did not have a significant influence on the network performance. However, the stability of the network system

exhibited moderate state conditions as the earthquake magnitude increased to 7.0. Specifically, when the earthquake magnitude was 7.0 and after 20 years of elapsed time, the CL and SR entered the major
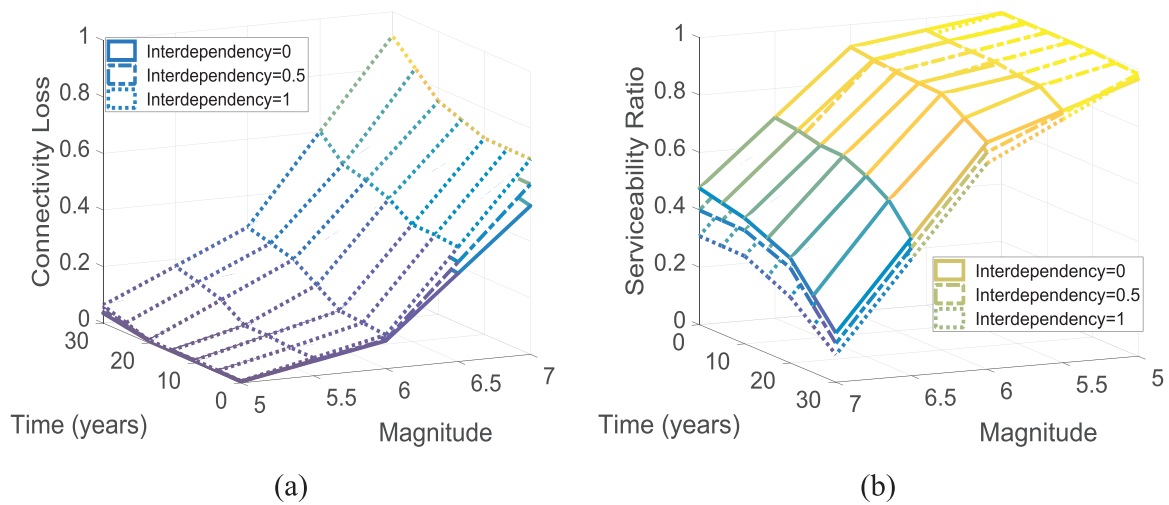
(a)

(b)

Fig. 13. Fragility surface of water transmission network considering interdependency of substation (source 1-sink connectivity) (a) CL (b) SR.
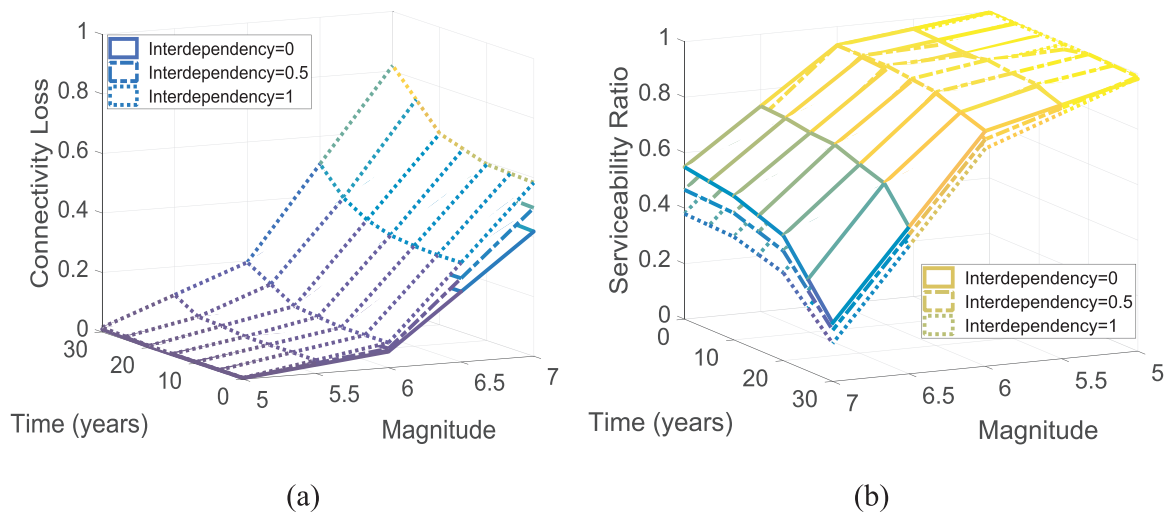

(a)

(b)

Fig. 14. Fragility surface of water transmission network considering interdependency of substation (source 2-sink connectivity): (a) CL, and (b) SR.
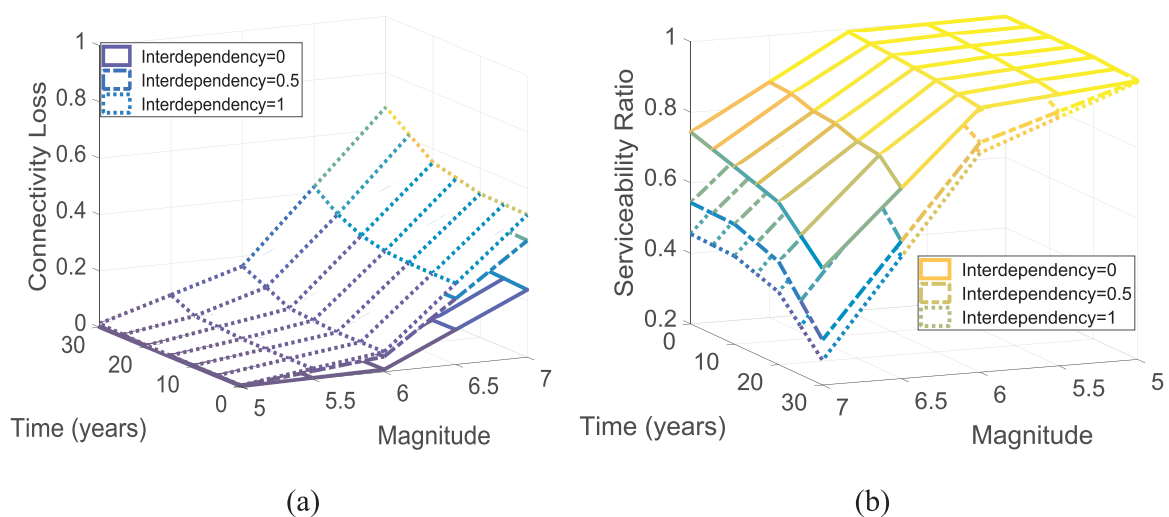

(a)

(b)

Fig. 15. Fragility surface of water transmission network considering interdependency of substation (two sources-sink connectivity): (a) CL, and (b) SR.

damage state conditions where 80% of the storage tanks cannot be supplied with water from water treatment plants. This is because 90% of the A-city water network comprises cast iron pipes, and the

probability of pipe survival declines significantly after 20–30 years (see Fig. 2). Another reason is that the seismic criteria of the South Korean water pipe is designed around magnitude 6.0 earthquakes, that is

related to the length of pipelines and the corresponding PGV intensity in Eq. (8). Therefore, it is possible to improve seismic performance when controlling the length of the pipelines. The first case study showed that it is essential to consider not only the characteristic of the epicenter (location and magnitude), but also the buried time of the pipeline, when evaluating a water network system.

In the second case study, the network response considering electric power substations was performed with conditional probability among the interdependent facilities. The effect of interdependency was not significant in earthquakes with a magnitude of 5.0 and 6.0, but the performance of interdependent networks decreased significantly as the magnitude of the earthquake increased to 7.0. As the earthquake magnitude and the elapsed time after being buried increased, the network performance from the interdependency decreased significantly. This was because the impact of the interdependency was greater for larger ground motions than for smaller ground motions, as shown in Fig. 5. In summary, for an earthquake of magnitude is 7.0, the maximum PGA of the pipelines was approximately 0.4 g. On the other hand, the maximum PGA of pipelines were 0.15 g and 0.08 g for earthquake magnitudes of 6.0 and 5.0, respectively. Therefore, a numerical analysis considering proper interdependency is required to predict the actual damage of network systems.

6. Conclusion

This study proposed a comprehensive framework for seismic risk assessment of urban water transmission networks. It provided guidelines for accurately predicting damage states to the network system from earthquakes. In order to evaluate the seismic risk assessment of network systems, the following issues were considered.

- A spatially correlated attenuation law was adopted for the uncertainty of ground motion.
- The results of a survival analysis were used to consider the deterioration of buried pipelines
- The interdependency effect among the facilities (water treatment plant, pumping plant, and substation) was taken into account.
- Two performance indicators (CL and SR) were measured for different earthquake magnitudes and elapsed times.

Results of numerical simulation shows that with increasing earthquake magnitude and elapsed time of pipeline, the depth of the CL fragility surface increased, however, the SR fragility surface decreased. Especially when the magnitude of earthquake was more than 7 and after 20 years of elapsed time, there was a great disruption of water supply. Furthermore, the interdependency among the electric power substation, water treatment plant, and water pumping station has a significant effects on water network. Even in the same earthquake magnitude and elapsed time, as the interdependence increases, the seismic risk of water network tends to be more vulnerable against earthquakes.

This study investigated a number of factors that affect the seismic resilience of water transmission networks that is related to pre-earthquake damage predictions. In order to improve the proposed comprehensive framework, the post-earthquake strategies should be improved and added to in the future. These strategies should include decision making of repair priority of pipelines, mitigation actions by using bypass or alternative routes, and emergency plans for water transmission networks. In addition, models for water distribution piping systems, such as EPANET, can be adopted to consider the customer demand satisfaction of urban areas, and numerous failure modes and damage states of liquid buried pipeline can also be taken into account.

Acknowledgements

References

[1] J. Kim, A. Deshmukh, M. Hastak, A framework for assessing the resilience of a disaster debris management system, Int. J. Disaster Risk Reduct. 28 (2018) 674–687.

[2] V. Cerchiello, P. Ceresa, R. Monteiro, N. Komendantova, Assessment of social vulnerability to seismic hazard in Nablus, Palestine, Int. J. Disaster Risk Reduct. 28 (2018) 491–506.

[3] PAHO (Pan American Health Organization), Emergencies and Disasters in Drinking Water Supply and Sewage Systems: Guidelines for Effective Response, 104 Regional office of the World Health Organization (WHO), Washington, DC, 2002.

[4] D.H. Lee, B.H. Kim, H. Lee, J.S. Kong, Seismic behavior of a buried gas pipeline under earthquake excitations, Eng. Struct. 31 (5) (2009) 1011–1023.

[5] D.G. Yoo, D. Jung, D. Kang, J.H. Kim, K. Lansey, Seismic hazard assessment model for urban water supply networks, J. Water Resour. Plan. Manag. 142 (2) (2015) 04015055.

[6] S.-S. Jeon, T.D. O'Rourke, Northridge earthquake effects on pipelines and residential buildings, Bull. Seismol. Soc. Am. 95 (1) (2005) 294–318.

[7] C. Nuti, A. Rasulo, I. Vanzi, Seismic safety of network structures and infrastructures, Struct. Infrastruct. Eng. 6 (1–2) (2010) 95–110.

[8] C. Nuti, A. Rasulo, I. Vanzi, Seismic assessment of utility systems: Application to water, electric power and transportation networks safety, reliability and risk analysis: Theory, methods and applications, in: Proceedings of the Joint ESREL and SRA-Europe Conference. 2009, pp. 2519–2529.

[9] C. Nuti, A. Rasulo, I. Vanzi, Seismic safety evaluation of electric power supply at urban level, Earthq. Eng. Struct. Dyn. 36 (2) (2007) 245–263.

[10] S. Esposito, I. Iervolino, A. d'Onofrio, A. Santo, F. Cavalieri, P. Franchin, Simulation-based seismic risk assessment of gas distribution networks, Comput. Aided Civ. Infrastruct. Eng. 30 (7) (2015) 508–523.

[11] K. Rokneddin, J. Ghosh, L. Dueñas-Osorio, J.E. Padgett, Bridge retrofit prioritisation for ageing transportation networks subject to seismic hazards, Struct. Infrastruct. Eng. 9 (10) (2013) 1050–1066.

[12] J. Ching, W.C. Hsu, An efficient method for evaluating origin-destination connectivity reliability of real-world lifeline, Netw., Comput. Aided Civ. Infrastruct. Eng. 22 (8) (2007) 584–596.

[13] M. Fragiadakis, S.E. Christodoulou, Seismic reliability assessment of urban water networks, Earthq. Eng. Struct. Dyn. 43 (3) (2014) 357–374.

[14] M. Fragiadakis, S.E. Christodoulou, D. Vamvatsikos, Reliability assessment of urban water distribution networks under seismic loads, Water Resour. Manag. 27 (10) (2013) 3739–3764.

[15] S. Christodoulou, M. Fragiadakis, A. Agathokleous, S. Xanthos, Urban Water Distribution Networks: Assessing Systems Vulnerabilities, Failures, and Risks, Butterworth-Heinemann, 2017.

[16] L. Dueñas-Osorio, J.I. Craig, B.J. Goodno, Seismic response of critical interdependent networks, Earthq. Eng. Struct. Dyn. 36 (2) (2007) 285–306.

[17] K. Poljanšek, F. Bono, E. Gutiérrez, Seismic risk assessment of interdependent critical infrastructure systems: the case of European gas and electricity networks, Earthq. Eng. Struct. Dyn. 41 (1) (2012) 61–79.

[18] Y.-J. Lee, J. Song, P. Gardoni, H.-W. Lim, Post-hazard flow capacity of bridge transportation network considering structural deterioration of bridges, Struct. Infrastruct. Eng. 7 (7–8) (2011) 509–521.

[19] W.-H. Kang, J. Song, P. Gardoni, Matrix-based system reliability method and applications to bridge networks, Reliab. Eng. Syst. Saf. 93 (11) (2008) 1584–1593.

[20] J. Song, W.-H. Kang, System reliability and sensitivity under statistical dependence by matrix-based system reliability method, Struct. Saf. 31 (2) (2009) 148–156.

[21] J. Song, S.Y. Ok, Multi-scale system reliability analysis of lifeline networks under earthquake hazards, Earthq. Eng. Struct. Dyn. 39 (3) (2010) 259–279.

[22] H.W. Lim, J. Song, Efficient risk assessment of lifeline networks under spatially correlated ground motions using selective recursive decomposition algorithm, Earthq. Eng. Struct. Dyn. 41 (13) (2012) 1861–1882.

[23] T. Adachi, B.R. Ellingwood, Serviceability of earthquake-damaged water systems: effects of electrical power availability and power backup systems on system vulnerability, Reliab. Eng. Syst. Saf. 93 (1) (2008) 78–88.

[24] S. Esposito, Systemic Seismic Risk Analysis of Gas Distribution Networks (Ph.D. thesis), University of Naples Fegerico II, 2011 (Ph. D. Program in SeismicRisk, Naples).

[25] N. Ambraseys, J. Douglas, S. Sarma, P. Smit, Equations for the estimation of strong ground motions from shallow crustal earthquakes using data from Europe and the middle East: horizontal peak ground acceleration and spectral acceleration, Bull. Earthq. Eng. 3 (1) (2005) 1–53.

[26] N.N. Ambraseys, J. Douglas, S.K. Sarma, P.M. Smit, Equations for the estimation of strong ground motions from shallow crustal earthquakes using data from Europe and the middle east: vertical peak ground acceleration and spectral acceleration, Bull. Earthq. Eng. 3 (1) (2005) 55–73.

[27] D.M. Boore, J.F. Gibbs, W.B. Joyner, J.C. Tinsley, D.J. Ponti, Estimated ground motion from the 1994 Northridge, California, earthquake at the site of the Interstate 10 and La Cienega Boulevard bridge collapse, West Los Angeles, California, Bull.

Seismol. Soc. Am. 93 (6) (2003) 2737–2751.

[28] N.A. Abrahamson, R. Youngs, A stable algorithm for regression analyses using the random effects model, Bull. Seismol. Soc. Am. 82 (1) (1992) 505–510.

[29] W.B. Joyner, D.M. Boore, Methods for regression analysis of strong-motion data, Bull. Seismol. Soc. Am. 83 (2) (1993) 469–487.

[30] K. Goda, H.-P. Hong, Spatial correlation of peak ground motions and response spectra, Bull. Seismol. Soc. Am. 98 (1) (2008) 354–365.

[31] M. Wang, T. Takada, Macrospatial correlation model of seismic ground motions, Earthq. Spectra 21 (4) (2005) 1137–1156.

[32] K. Kawashima, K. Aizawa, K. Takahashi, Attenuation of peak ground motion and absolute acceleration response spectra, in: Proceedings of the Eighth World Conference on Earthquake Engineering, 1984, pp. 257–264.

[33] T. Wagener, K. Goda, M. Erdik, J. Daniell, F. Wenzel, A spatial correlation model of peak ground acceleration and response spectra based on data of the Istanbul earthquake rapid response and early warning system, Soil Dyn. Earthq. Eng. 85 (2016) 166–178.

[34] G.P. Cimellaro, A. De Stefano, A.M. Reinhorn, Intra-event spatial correlation of ground motion using L'Aquila earthquake ground motion data, in: Proceedings of the 3rd ECCOMAS Thematic Conference on Computational Methods in Structural Dynamics and Earthquake Engineering, Corfu, Greece, 2011, pp. 3091–3108.

[35] S. Esposito, I. Iervolino, Spatial correlation of spectral acceleration in European data, Bull. Seismol. Soc. Am. 102 (6) (2012) 2781–2788.

[36] V. Sokolov, F. Wenzel, W.-Y. Jean, K.-L. Wen, Uncertainty and spatial correlation of earthquake ground motion in Taiwan, Terr. Atmos. Ocean. Sci. (2010).

[37] K. Goda, G.M. Atkinson, Probabilistic characterization of spatially correlated response spectra for earthquakes in Japan, Bull. Seismol. Soc. Am. 99 (5) (2009) 3003–3020.

[38] K. Goda, G.M. Atkinson, Intraevent spatial correlation of ground-motion parameters using SK-net data, Bull. Seismol. Soc. Am. 100 (6) (2010) 3055–3067.

[39] FEMA, HAZUS-MH-MR3 technical manual: In Multi-Hazard Loss Estimation Methodology Earthquake Model, United States Department of Homeland Security, Federal Emergency Management Agency, Washington, DC, 2003.

[40] ALA, Seismic Fragility Formulations for Water Systems Guideline and Appendices, American Lifelines Alliance, Washington, DC, 2001.

[41] D.B. Ballantyne, Earthquake loss estimation modeling of the Seattle water system: Technical Report 886005, supported by U.S. Geological Survey Project Number 14-08-0001-G1526, Kennedy/Jenks/Chilton, 1990.

[42] G. Lanzano, F.S. de Magistris, G. Fabbrocino, E. Salzano, Seismic damage to pipelines in the framework of Na-Tech risk assessment, J. Loss Prev. Proc. Ind. 33 (2015) 159–172.

[43] G. Lanzano, E. Salzano, F.S. De Magistris, G. Fabbrocino, Seismic vulnerability of gas and liquid buried pipelines, J. Loss Prev. Proc. Ind. 28 (2014) 72–78.

[44] A. Panico, A. Basco, G. Lanzano, F. Pirozzi, F.S. de Magistris, G. Fabbrocino, E. Salzano, Evaluating the structural priorities for the seismic vulnerability of civilian and industrial wastewater treatment plants, Saf. Sci. 97 (2017) 51–57.

[45] J. Hintz, NCSS and PASS. Number Cruncher Statistical Systems. Kaysville, Utah, 2001.

[46] D.W. Hosmer, S. Lemeshow, S. May, Applied Survival Analysis, Wiley Blackwell, 2011.

[47] S. Christodoulou, A. Deligianni, A neurofuzzy decision framework for the management of water distribution networks, Water Resour. Manag. 24 (1) (2010) 139–156.

[48] S.E. Christodoulou, Water network assessment and reliability analysis by use of survival analysis, Water Resour. Manag. 25 (4) (2011) 1229–1238.

[49] S. Park, C.L. Choi, J.H. Kim, C.H. Bae, Evaluating the economic residual life of water pipes using the proportional hazards model, Water Resour. Manag. 24 (12) (2010) 3195–3217.

[50] V. Latora, M. Marchiori, Vulnerability and protection of infrastructure networks, Phys. Rev. E 71 (1) (2005) 015103.

[51] Y. Wang, S.-K. Au, Q. Fu, Seismic risk assessment and mitigation of water supply systems, Earthq. Spectra 26 (1) (2010) 257–274.

[52] M. Javanbarg, C. Scawthorn, J. Kiyono, Y. Ono, Minimal path sets seismic reliability evaluation of lifeline networks with link and node failures, TCLEE 2009: Lifeline Earthq. Eng. a Multihazard Environ. (2009) 1–12.

[53] J.E. Ramirez-Marquez, D.W. Coit, A Monte-Carlo simulation approach for approximating multi-state two-terminal reliability, Reliab. Eng. Syst. Saf. 87 (2) (2005) 253–264.

[54] J.E. Gentle, Random Number Generation and Monte Carlo Methods, Springer Science & Business Media, 2006.

[55] L. Devroye, Non-Uniform Random Variate Generation, Springer-Verlag, New York, 1986.

[56] S. Even, R.E. Tarjan, Network flow and testing graph connectivity, SIAM J. Comput. 4 (4) (1975) 507–518.

[57] N.P. Hummon, P. Doreian, Computational methods for social network analysis, Soc. Netw. 12 (4) (1990) 273–288.

[58] G. Rubino, B. Tuffin, Rare Event Simulation Using Monte Carlo Methods, John Wiley & Sons, 2009.